# Stepwise hydration of the cyanide anion: A temperature-controlled photoelectron spectroscopy and *ab initio* computational study of $CN^-(H_2O)_n$, $n=2-5$

Xue-Bin Wang,[1,a)] Karol Kowalski,[2] Lai-Sheng Wang,[3] and Sotiris S. Xantheas[4,b)]
[1]*Department of Physics, Washington State University, 2710 University Drive, Richland, Washington 99354, USA and Chemical and Materials Sciences Division, Pacific Northwest National Laboratory, P.O. Box 999, MS K8-88, Richland, Washington 99352, USA*
[2]*Environmental Molecular Sciences Laboratory, Pacific Northwest National Laboratory, P.O. Box 999, MS K8-91, Richland, Washington 99352, USA*
[3]*Department of Chemistry, Brown University, Providence, Rhode Island 02912, USA*
[4]*Chemical and Materials Sciences Division, Pacific Northwest National Laboratory, 902 Battelle Boulevard, P.O. Box 999, MS K1-83, Richland, Washington 99352, USA*

(Received 18 November 2009; accepted 22 February 2010; published online 30 March 2010)

We report the study of microsolvated $CN^-(H_2O)_n$ ($n=1-5$) clusters in the gas phase using a combination of experimental and computational approaches. The hydrated cyanide clusters were produced by electrospray and their structural and energetic properties were probed using temperature-controlled photoelectron spectroscopy (PES) and *ab initio* electronic structure calculations. Comparison between the low temperature (LT,T=12 K) and the room-temperature (RT) spectra shows a 0.25 eV spectral blueshift in the binding energy of the $n=1$ cluster and a significant spectral sharpening and blueshift for $n=2$ and 3. The experimental results are complemented with *ab initio* electronic structure calculations at the MP2 and CCSD(T) levels of theory that identified several isomers on the ground state potential energy function arising from the ability of $CN^-$ to form hydrogen bonds with water via both the C and N ends. In all cases the N end seems to be the preferred hydration site for the water network. The excellent agreement between the low temperature measured PES spectra and the basis set- and correlation-corrected [at the CCSD(T) level of theory] calculated vertical detachment energies, viz., 3.85 versus 3.84 eV ($n=0$), 4.54 versus 4.54 eV ($n=1$), 5.20 versus 5.32 eV ($n=2$), 5.58 versus 5.50 eV ($n=3$), and 5.89 versus 5.87 eV ($n=4$), allow us to establish the hydration motif of cyanide. Its microsolvation pattern was found to be similar to that of the halide anions ($Cl^-$, $Br^-$, and $I^-$) as well as other diatomic anions having cylindrical symmetry such as $NO^-$, resulting to structures in which the ion resides on the surface of a water cluster. The exception is $CN^-(H_2O)_2$, for which one water molecule is bound to either side of the anion resulting in a quasilinear structure. For the $n=3$ cluster the anion was found to freely "tumble" on the surface of a water trimer, since the inclusion of zero-point energy even at T=0 K stabilizes the configuration of $C_3$ symmetry with respect to the one having the anion tilted toward the water cluster. For $n=4$ this motion is more restricted since the corresponding barrier at RT is 1.2 kcal/mol. It is also possible that at RT other isomers (lying within ~0.6 kcal/mol above the global minima) are also populated, resulting in the further broadening of the PES spectra. © *2010 American Institute of Physics*. [doi:10.1063/1.3360306]

## I. INTRODUCTION

Gaseous clusters with a controlled number of solvent molecules are ideal model systems for providing a fundamental understanding of solute-solvent and solvent-solvent interactions at the molecular level. Cyanide ($CN^-$) is an important complex anion, present ubiquitously in solutions and solids, and has wide applications in coordination chemistry and materials science.[1] Extensive studies on the thermodynamic and spectroscopic properties of the bare $CN^-$,[2–5] its molecular properties in crystals,[6,7] and the dynamics of vibration energy transfer in solutions[8–12] have been previously reported. Its hydration and clustering with HCN have been investigated using high-pressure mass spectrometric equilibrium methods,[13–16] as well as theoretical calculations.[15–19] $CN^-$ has many chemical and physical properties similar to $Cl^-$ in many aspects, i.e., ionic radius (being only slightly larger),[16] polarizability (3.83 versus 3.69 Å$^3$),[6,20] electron binding energy (3.862 versus 3.612 eV),[2,21] and hydration energy (13.8 versus 13.1 kcal/mol).[13] Despite its fame as a "pseudohalide," the cyanide anion displays distinctly different behavior from the halides in its hydration mechanism because it is an ellipsoidal instead of a spherical ion, and can therefore form two nearly isoenergetic H-bonded complexes with water via either the C or N side,[15,17,19] as has been previously suggested by Lee.[17] To date, a fundamental understanding of the interaction of $CN^-$ with water at the mo-

a)Electronic mail: xuebin.wang@pnl.gov.
b)Electronic mail: sotiris.xantheas@pnl.gov.

 

lecular level is still limited.[22] Clearly, such information is desirable in order to understand its physical properties and chemical processes in condensed environments.

Gas phase spectroscopic studies of solvated clusters are an important vehicle that can be used to obtain microscopic insights into the solution phase.[23–31] The structures and energetics of hydrated clusters with the first few water molecules are of particular importance since they provide quantitative information of the delicate balance between the ion-water and water-water interactions and can serve as prototypes to understand larger clusters and the behavior of the ions in the bulk. Many gas phase techniques, ion cooling schemes, as well as theoretical methods have been previously developed in order to investigate solvated species of primarily simple,[24–34] as well as diatomic solute ions.[35–40] The electrospray ionization (ESI) technique has allowed recent advances in the investigation of more complex ions.[41–45] Low-temperature and temperature-dependent studies are particularly valuable for the study of the solvation of complex ions. These studies can eliminate hot bands and stabilize weakly bound species or different conformers,[46,47] as well as unravel critical entropic effects and isomer populations as a function of temperature.[44,45] In contrast to previous extensive experimental and theoretical studies of the $Cl^-(H_2O)_n$ clusters,[30–34] and recent pioneering works on hydrated diatomic anionic clusters such as $O_2^-$,[35,36] $NO^-$[37], and $Cl_2^-$,[38] gas phase spectroscopic studies of $CN^-(H_2O)_n$ clusters have been very limited.[22] The study of $CN^-(H_2O)_n$ clusters can yield details about the microscopic molecular interactions between $CN^-$ and $H_2O$, providing a case for comparison with the solvation motifs of the halide and other diatomic anions.

Very recently we have reported a photoelectron spectroscopy (PES) study of the $CN^-(H_2O)$ monohydrate at T=12 K (LT) and room temperature (RT), and observed a surprisingly large spectral redshift of 0.25 eV at RT.[22] The accompanying analysis of the potential energy function (PEF) using *ab initio* calculations suggested that the water rocking (relative to $CN^-$) mode becomes accessible at RT. Thus the RT spectrum reflects, on average, a detachment process close to the transition state ($CN^-$ bisecting the H–O–H angle) relative to that from the $C_s$ global minima ($CN^-$ interacting with one H of $H_2O$ moiety), giving rise to the experimentally observed spectral shift. Interestingly, a similar mechanism can be used to interpret the apparently different infrared action spectra of $Cl^-(H_2O)$ reported earlier by Okumura *et al.* at RT (Ref. 30) and by Johnson *et al.* at low temperatures.[31] In these studies, similar vibrational frequencies were observed, but the respective intensities were completely different due to the fact that the clusters can access different parts of the PEF at different temperatures.

In this paper we extend our previous joint experimental/theoretical study of the $CN^-(H_2O)$ monohydrate to the larger $CN^-(H_2O)_n$, $n=2-5$, clusters. PES spectra were obtained at two temperatures (T=12 K and RT) for the $n=1-3$ clusters and at T=12 K for the $n=4$ and 5 clusters. The comparison between the LT and RT spectra revealed a significant spectral sharpening for $n=2$ and 3, in addition to the spectral blueshift previously reported for $n=1$.[22] High level *ab initio* calculations at the MP2 and CCSD(T) levels of theory identified the global minimum for each cluster and suggested two sets of close lying isomers corresponding to $CN^-(H_2O)_n$ and $NC^-(H_2O)_n$ with the N and C ends primarily interacting with a water cluster, respectively. The calculated vertical detachment energies (VDEs) are found to be sensitive to the cluster structures, and the calculated VDEs of the global minima are in excellent agreement with the measured experimental data at LT. The observed spectral broadening on the low binding energy side for $n=2$ and 3 at RT are attributed to the population of low-lying isomers that have lower VDEs. The solvation pattern of $CN^-$ is compared and discussed with reference to hydration patterns of $Cl^-$ and other diatomic anions.

## II. EXPERIMENTAL AND THEORETICAL METHODS

### A. Photoelectron spectroscopy

The LT PES spectra of the $CN^-(H_2O)_n$, $n=1-5$, clusters were obtained with a recently developed apparatus that couples an ESI source to a temperature-controlled Paul trap (10–350 K tunable range) and a magnetic-bottle time-of-flight (TOF) photoelectron spectrometer.[48] The RT experiment on the bare and small cluster anions ($n=0-3$) was carried out using an ESI-PES instrument that has been described in detail elsewhere.[49] The solvated $CN^-(H_2O)_n$, $n=0-5$, clusters were generated via electrospray from a 0.1 mM NaCN acetonitrilic aqueous solution (3:1 v/v). The resulting ions were guided by two rf-only quadrupole devices and then bent by 90° into a temperature-controlled three-dimensional Paul trap, where they were accumulated and cooled down before being pulsed into the extraction zone of a TOF mass spectrometer. In the current study the lowest temperature of 12 K was used. Studies at other intermediate temperatures are possible and will be pursued in the future.

In the subsequent PES experiments the clusters were mass-selected and decelerated before being detached by a 193 nm (6.424 eV) ArF excimer laser for the solvated clusters and a 266 nm (4.661 eV) Nd:YAG (neodymium-doped yttrium aluminum garnet) laser for the bare ion in the interaction zone of a magnetic-bottle photoelectron analyzer. The laser was operated at a 20 Hz repetition rate with the ion beam off on alternating laser shots for background subtraction. Photoelectrons were collected at nearly 100% efficiency by the magnetic bottle and analyzed in a 5.2 m long electron flight tube. TOF photoelectron spectra were collected and converted to kinetic energy spectra calibrated using the known spectra of $I^-$ and $ClO_2^-$. The electron binding energy spectrum reported herein was obtained by subtracting the kinetic energy spectrum from the detachment photon energy. The energy resolution ($\Delta E/E$) of the magnetic-bottle electron analyzer was 2% (i.e., 20 meV for 1 eV electrons).

### B. Electronic structure calculations

We anticipate that there would be different theoretical requirements as regards to the level of *ab initio* theory needed to obtain (i) the relative energetics of the various cluster isomers and therefore be able to predict the global minimum for each cluster and (ii) the corresponding VDEs, which can be directly compared with the experiment, as the

latter involve additional calculations on the PEF of the neutral $CN(H_2O)_n$ clusters. Given the fact that extensive searches on multidimensional PEFs are needed to determine the isomers of clusters of $CN^-$ with as many as 5 water molecules, it is desirable to use a lower level of theory for the geometry optimizations and subsequently correct the relative energetics and VDEs at a higher level of theory. In our previous study[22] we have used the experimentally obtained VDEs for $CN^-$ and the monohydrate $CN^-(H_2O)$ cluster as benchmarks in order to calibrate the accuracy of different levels of *ab initio* theory that included the second order Moller–Plesset (MP2) and coupled-cluster singles and doubles with perturbative estimate of triple excitations [CCSD(T)] in conjunction with the family of augmented correlation consistent basis sets, aug-cc-pV*n*Z ($n$=D, T, Q) of Dunning and co-workers.[50] The results of our previous study for the $n=0,1$ clusters suggested that (i) the calculated VDEs increased monotonically with the size of the basis set at both the MP2 and CCSD(T) levels of theory, (ii) the CCSD(T) method produces very accurate VDEs: the results obtained at the CCSD(T)/aug-cc-pVQZ level of theory are within 0.02 eV from the experimentally measured ones, (iii) the MP2 method overestimates the experimentally measured VDEs by as much as 0.5 eV: the results obtained at the MP2/aug-cc-pVQZ level overestimated the experimental ones by ~0.5 eV and finally (iv) the CCSD(T)/aug-cc-pVDZ VDEs are 0.2 eV *smaller* than the experimentally measured values and/or the CCSD(T)/CBS limit [since CCSD(T) numbers converge from below, see point (i)], whereas the MP2/aug-cc-pVDZ VDEs are ~0.3 eV *larger* than experiment (since MP2 overestimates the VDEs, see points (i) and (iii)].

Given those findings we have adopted the following computational strategy: for $n=2$ all minima (isomers) were fully optimized at both the MP2 and CCSD(T) levels of theory with the aug-cc-pVDZ basis set. For $n=3,4$, the minima were optimized at the MP2/aug-cc-pVDZ level and subsequent single point energy calculations were run at the CCSD(T)/aug-cc-pVDZ level at the MP2 optimal geometries. All MP2 calculations were performed with the Gaussian 98 suite of codes,[51] whereas all CCSD(T) calculations were carried out with the NWCHEM suite of electronic structure codes.[52] All open-shell coupled-cluster calculations, needed for the calculation of the VDEs (calculated as the energy difference between the optimized anionic structure and that of the corresponding neutral at the anionic geometry), were based on a doublet restricted open-shell Hartree–Fock reference with the core electrons being frozen. These calculations were performed using the tuned Tensor Contraction Engine (TCE) (Ref. 53) implementation of the CCSD [Ref. 54(a)] and CCSD(T) approaches[54(b)] implemented within the NWCHEM suite of electronic structure codes.[52] Zero-point energy (ZPE) corrections were estimated at the harmonic approximation.

## III. EXPERIMENTAL RESULTS

### A. ESI mass spectrum

The $CN^-(H_2O)_n$ ($n=0-6$) clusters were generated via spraying of a 0.1 mM NaCN aqueous acetonitrilic solution.

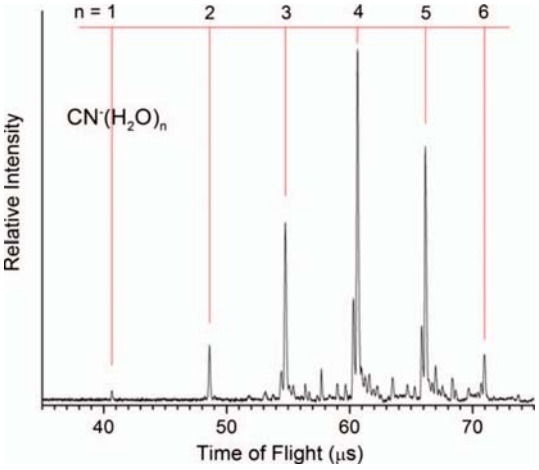


FIG. 1. TOF mass spectrum of $CN^-(H_2O)_n$, $n=1-6$, generated via the electrospray of a $10^{-4}$ M NaCN in $H_2O/CH_3CN$ (1/3 volume ratio) solution.

The source conditions, particularly the water vapor pressure, and a series of electrostatic ion-optical lens voltages along the ion transport path were optimized to maximize each species. Figure 1 shows a typical TOF mass spectrum optimized for $n=4$. Overall, the intensity of the hydrated species is weak, especially for the larger ($n\geq 6$) clusters.

### B. Low temperature photoelectron spectra

The T=12 K PES spectra of $CN^-(H_2O)_n$ ($n=1-5$) at 193 nm are shown in Fig. 2 (blue). The spectrum for $n=1$ was published earlier[22] but is included here for completeness. The 266 nm spectrum of bare $CN^-$ is also included with a measured peak position of 3.85 eV, compared with 3.862 eV from a previous high-resolution study.[2] The $CN^-$ spectrum confirmed the proper calibrations under which the hydrated cluster spectra were taken. The PES spectra of all

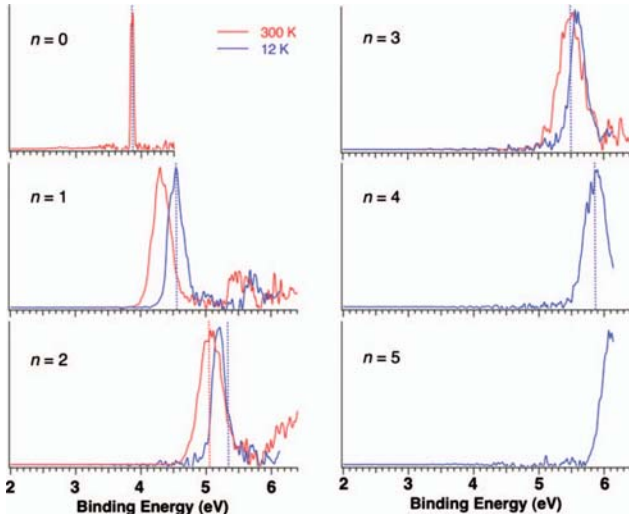


FIG. 2. Photoelectron spectra of $CN^-(H_2O)_n$ at 266 nm (4.661 eV, $n=0$), 193 nm (6.424 eV, $n=1-5$) under RT (red), and T=12 K (blue) trap temperatures. The calculated VDEs at the CCSD(t)/aug-cc-pVQZ ($n=0,1$) and *basis-set-corrected* CCSD(t)/aug-cc-pVDZ ($n=2$, 3, and 4) are shown as vertical broken lines in blue and red for the global minima and the low-lying isomers, respectively. The spectra of $n=1$ was published earlier (Ref. 22) and it is included here for completeness.

TABLE I. Minimum energies (a.u.) of the optimized geometries of the anionic clusters $CN^-(H_2O)_n$ and single point energies of the corresponding neutral species, relative energies (kcal/mol) of the $CN^-(H_2O)_n$ and $NC^-(H_2O)_n$ isomers (including harmonic ZPE corrections in parentheses), calculated VDEs (eV), and their comparison with experimentally measured values obtained at T=12 K and RT (in parentheses).

| Species | Level of theory | Basis set | Anion (a.u.) | $\Delta\Delta E_e$ ($\Delta\Delta E_0$) (kcal/mol) | Neutral (a.u.) | VDE (Calc.) (eV) | VDE (Expt) (eV) |
|---|---|---|---|---|---|---|---|
| 2-I, linear | MP2 | aug-cc-pVDZ | −245.191 078 | 0 (0) | −244.985 810 | 5.59 | |
| | | | | | | | **5.20±0.05** |
| | CCSD(T) | aug-cc-pVDZ | −245.236 078 | 0 (0) | −245.048 655 | **5.10** | (5.10±0.08) |
| | CCSD(T) | aug-cc-pVDZ @MP2/aug-cc-pVDZ geometry | −245.235 965 | 0 | −245.047 725 | **5.12** | |
| 2-II, CN-c | MP2 | aug-cc-pVDZ | −245.190 172 | 0.57 (1.34) | −244.997 716 | 5.24 | |
| | CCSD(T) | aug-cc-pVDZ | −245.235 923 | 0.10 (0.61) | −245.058 013 | **4.84** | |
| | CCSD(T) | aug-cc-pVDZ @MP2/aug-cc-pVDZ geometry | −245.235 844 | 0.08 | −245.057 136 | **4.86** | |
| 2-III, NC-c | MP2 | aug-cc-pVDZ | −245.189 682 | 0.88 (1.51) | −244.985 070 | 5.57 | |
| | CCSD(T) | aug-cc-pVDZ | −245.234 662 | 0.89 (1.47) | −245.050 867 | 5.00 | |
| | CCSD(T) | aug-cc-pVDZ @MP2/aug-cc-pVDZ geometry | −245.234 528 | 0.90 | −245.049 814 | **5.03** | |
| | | | | | | | **5.58±0.08** |
| 3-I, pyr. | MP2 | aug-cc-pVDZ | −321.474 363 | 0 (0) | −321.263 279 | 5.74 | (5.50±0.10) |
| | CCSD(T) | aug-cc-pVDZ @MP2/aug-cc-pVDZ geometry | −321.532 994 | ··· | −321.338 403 | **5.30** | |
| 3-II, CN-r | MP2 | aug-cc-pVDZ | −321.472 326 | 1.28 (0.60) | −321.264 630 | **5.65** | |
| 3-III, CN-p/r | MP2 | aug-cc-pVDZ | −321.470 559 | 2.39 (1.36) | −321.262 227 | 5.67 | |
| 3-IV, NC-r | MP2 | aug-cc-pVDZ | −321.470 714 | 2.29 (1.40) | −321.257 220 | 5.81 | |
| 3-V, NC-p/r | MP2 | aug-cc-pVDZ | −321.469 685 | 2.94 (1.62) | −321.255 905 | 5.82 | |
| 4-I, pyr. | MP2 | aug-cc-pVDZ | −397.759 350 | 0 (0) | −397.533 879 | 6.14 | **5.89±0.08** |
| | CCSD(T) | aug-cc-pVDZ @MP2/aug-cc-pVDZ geometry | −397.830 967 | ··· | −397.622 484 | **5.67** | |
| 4-II, NC-/3+1 | MP2 | aug-cc-pVDZ | −397.755 532 | 2.40 (1.39) | −397.523 110 | 6.32 | |
| 4-III, CN-/3+1 | MP2 | aug-cc-pVDZ | −397.755 283 | 2.55 (1.49) | −397.526 088 | 6.24 | |
| $CN^-(H_2O)_5$ | | | | | | | **6.09±0.08** |

species are similar, each exhibiting one strong peak with monotonically increased binding energy as the cluster size increases. For $n=5$ this feature is only partially observed due to the photon energy limit (6.424 eV) and a systematic spectral shift to higher electron binding energies. The relatively weak feature at ~5.7 eV observed for $n=1$ is due to the transitions to the excited states of the neutral.[22] This feature is missing for all larger clusters, except from the RT spectrum of the $n=2$ cluster, because of the expected high binding energies. The apparent broadening of the spectral width for the clusters compared with the atomiclike transition for the bare $CN^-$ anion is due to solvent relaxation upon electron detachment.

The solvation effect and the solvent stabilization are manifested as the spectrum of each species systematically shifts to high binding energies with increasing $n$. The VDEs measured from the T=12 K spectra are 4.54, 5.20, 5.58, 5.89, and 6.09 eV for $n=1-5$ (Table I), yielding stepwise stabilization energies [defined as $\Delta VDE(n)=VDE(n)-VDE(n-1)$] of 0.69, 0.66, 0.38, 0.31, and 0.2 eV for $n=1-5$, respectively. The first two water molecules are found to induce a much more significant stabilization effect on $CN^-$ than the additional water molecules.

As we reported previously,[22] the major observation of the RT spectrum of the $n=1$ cluster is a large spectral redshift of ~0.25 eV, while the spectral width is only marginally broader. This spectral shift originates from the accessibility of the water rocking vibrational hot bands at RT. Therefore the RT spectrum largely reflects a detachment process from configurations resembling the transition state rather than the global minimum (the latter being the case for LT). In contrast, the RT spectra of the $CN^-(H_2O)_2$ and $CN^-(H_2O)_3$ clusters show significant spectral broadening to the low binding energy side besides sizable spectral redshifts (~0.10, and 0.08 eV for $n=2$, and 3, respectively, cf. Table I), while the edges at the high binding energy side remain largely unaffected when compared with the LT spectral features.

## IV. THEORETICAL RESULTS

First principles electronic structure calculations were performed in order to identify the various cluster isomers and compute the corresponding VDEs in order to compare with the experimental spectra. We have recently reported extensive theoretical calculations for $CN^-$ and the $CN^-(H_2O)$ cluster at the MP2 and CCSD(T) levels of theory using the family of augmented correlation consistent (aug-cc-pV*n*Z, $n$=D, T, and Q) basis sets.[22] For the larger ($n\geq 2$) clusters, we have started the geometry optimizations from several chemically different structures in order to locate the various minima without using any symmetry. The total binding energies of the $n=1-4$ clusters are listed in Table II. The corresponding optimized structures of the global and the low-lying local

TABLE II. Absolute binding energies (kcal/mol) of the small cyanide—water clusters. All results shown are obtained with the aug-cc-pVDZ basis set.

| Species | Isomer | Level of theory | $\Delta E_e$ (kcal/mol) |
|---|---|---|---|
| $CN^-(H_2O)$ | $CN^-(H_2O)$ | MP2 | −15.96 |
| | | CCSD(T) | −15.82 |
| | $NC^-(H_2O)$ | MP2 | −15.86 |
| | | CCSD(T) | −15.43 |
| $CN^-(H_2O)_2$ | (2-I) linear | MP2 | −30.46 |
| | | CCSD(T) | −29.96 |
| | (2-II) CN-cyclic | MP2 | −29.90 |
| | | CCSD(T) | −29.86 |
| | (2-III) NC-cyclic | MP2 | −29.59 |
| | | CCSD(T) | −29.07 |
| $CN^-(H_2O)_3$ | (3-I) pyramidal | MP2 | −44.50 |
| | (3-II) CN-ring | MP2 | −43.23 |
| | (3-III) CN-pyr./ring | MP2 | −42.12 |
| | (3-IV) NC-ring | MP2 | −42.21 |
| | (3-V) NC-pyr./ring | MP2 | −41.57 |
| $CN^-(H_2O)_4$ | (4-I) pyramidal | MP2 | −59.61 |
| | (4-II) NC-/3+1 | MP2 | −57.22 |
| | (4-III) CN-/3+1 | MP2 | −57.06 |

minima are shown in Figs. 3–5 for the $n=2-4$ clusters, respectively, and their relative energies and calculated VDEs are listed in Table I along with the experimental data for comparison. In the following we discuss the structural motifs of the $n=2-4$ clusters.

### A. $CN^-(H_2O)_2$

Three low-lying isomers are identified for this species (Fig. 3). The global minimum corresponds to a structure that optimizes the $CN^-$ interactions with one H atom of the first water molecule via the N end and with another H atom of the second water molecule via the C end, resulting in an overall linear structure (2-I), in which no water-water hydrogen bonding exists and the two free OH bonds are in the *trans* position. The calculated VDE for the linear isomer [structure (2-I)] at the CCSD(T)/aug-cc-pVDZ level is 5.10 eV, just 0.1 eV smaller than the experimental result of 5.20 eV (Table I and Fig. 2). In contrast, the MP2/aug-cc-pVDZ VDE is 0.39 eV higher than the experimental value. This is consistent with our previous finding for the $CN^-$ and the $CN^-(H_2O)$ cluster,[22] that has been noted as point (*iv*) previously in Sec. II B. Furthermore the CCSD(T)/aug-cc-pVDZ//MP2/aug-cc-pVDZ VDE (i.e., the CCSD(T) VDE computed at the MP2 geometry) is 5.12 eV, just 0.02 eV away from the value obtained upon full geometry optimization at the CCSD(T) level. This suggests that the use of MP2 geometries to obtain VDEs at the CCSD(T) level by single point calculations

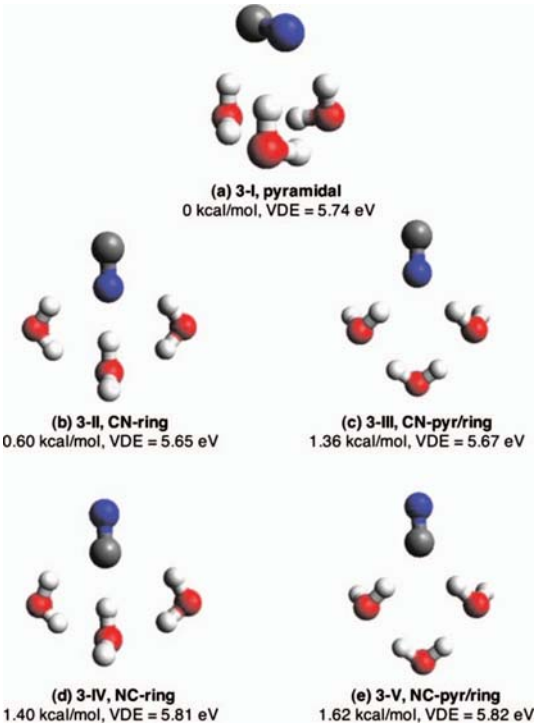


FIG. 4. Optimized structures, relative energies including zero-point energy corrections and VDEs for the low-lying energy isomers of $CN^-(H_2O)_3$ at the MP2/aug-cc-pVDZ level of theory.

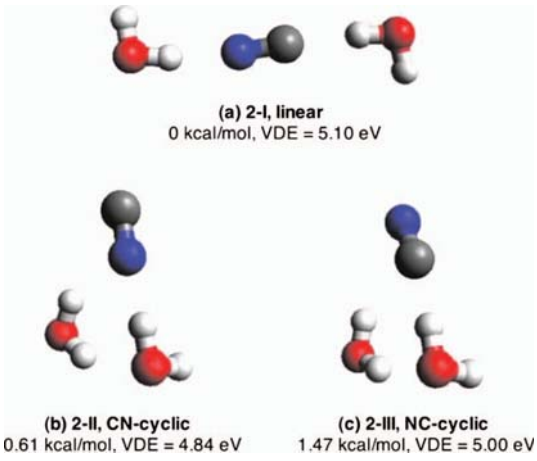


FIG. 3. Optimized (MP2/aug-cc-pVDZ) structures, relative energies including zero-point energy corrections and VDEs at CCSD(T)/aug-cc-pVDZ for the low-lying energy isomers of $CN^-(H_2O)_2$.

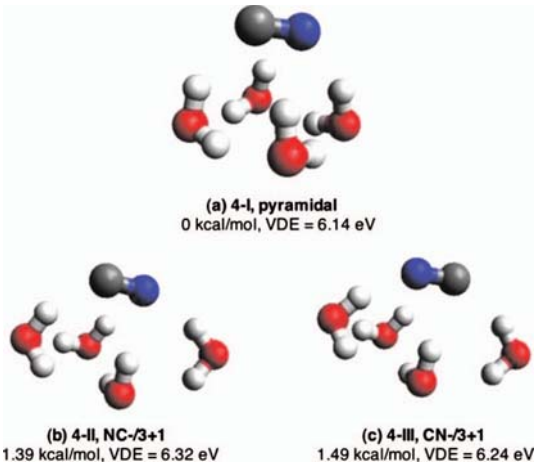


FIG. 5. Optimized structures, relative energies including zero-point energy corrections and VDEs for the low-lying energy isomers of $CN^-(H_2O)_4$ at the MP2/aug-cc-pVDZ level of theory.

yields quite accurate results because there is no appreciable geometry changes seem to occur upon going from MP2 to CCSD(T). The next low-lying isomer (2-II), which is 0.61 kcal/mol higher in energy than the (2-I) global minimum, corresponds to a cyclic structure where two water molecules each form one O–H···N with $CN^-$, as well as one interwater H-bond with one water molecule as the donor and the other as the acceptor (Fig. 3). The third isomer (2-III), which is 1.47 kcal/mol higher in energy than the global minimum, has an overall similar structure as (2-II) but with the $CN^-$ interacting with the two water molecules via the C end forming O–H···C hydrogen bonds. The CCSD(T)/aug-cc-pVDZ calculated VDEs are 4.84 eV (2-II) and 5.00 eV (2-III), respectively. There are also minimal changes (<0.03 eV) upon using the MP2 optimal geometries as was the case for the global minimum. The VDEs for the higher lying isomers (2-II) and (2-III) are both smaller than that of the global minimum (2-I). These results are consistent with the fact that the global minimum [isomer (2-I)] has a VDE that is closer than those for the other two isomers to the experimentally measured value when corrections for a larger basis set and electron correlation at the CCSD(T) level are taken into account.

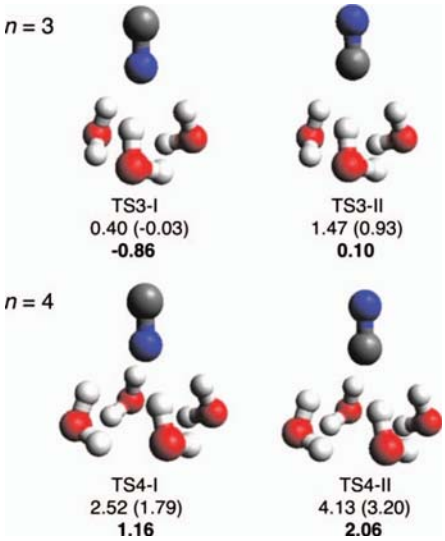


FIG. 6. Optimized structures and relative energies (kcal/mol) including zero-point energy corrections (in parentheses) for the symmetric transition states of the $n=3$ (TS3-I and TS3-II) and $n=4$ (TS4-I and TS4-II) clusters at the MP2/aug-cc-pVDZ level of theory. Enthalpy differences (kcal/mol) at T=298.15 K are also indicated in bold. The relative energetics are computed with respect to the most stable 3-I and 4-I isomers, respectively.

### B. $CN^-(H_2O)_3$

For this cluster we identified five minima (shown in Fig. 4) that are the consequence of the balance between solvent-solvent and ion-solvent interactions. The global minimum (3-I) adopts a three-water ring motif, with every water molecule acting as both a donor and an acceptor to its neighbor. The water portion of the global minimum resembles the (*uuu*) local minimum[55] (all "free" H atoms on the same side of the plane defined by the three Oxygen atoms) of the water trimer,[56] a water network that was first reported for the structure of the $H^-(H_2O)_3$ cluster[57] and subsequently for the $Cl^-(H_2O)_3$ (Ref. 33) and $OH^-(H_2O)_3$ (Ref. 58) clusters. The $CN^-$ ion lies almost parallel to the plane of the three Oxygen atoms and the structure having $C_3$ symmetry is a first order transition state (TS3-I in Fig. 6, N atom toward the water cluster) with an imaginary frequency of 46.4 $cm^{-1}$ (*E* symmetry) that lies 0.4 kcal/mol above the global minimum 3-I. However, inclusion of zero-point energy corrections suggests that (even at T=0 K) transition state TS3-I is 0.03 kcal/mol *below* 3-I. Furthermore at T=298 K the enthalpy of the TS3-I configuration is 0.86 kcal/mol below that of 3-I. The corresponding TS3-II (C atom toward the water cluster, cf. Fig. 6), which also has $C_3$ symmetry, lies 1.47 kcal/mol above 3-I on the PEF. When accounting for zero-point energy corrections, this difference reduces to 0.93 kcal/mol, whereas at T=298 K to 0.10 kcal/mol (3-I still lower in energy). These results suggest that there is a large amplitude vibration for the "tumbling" of $CN^-$ on the surface of the water network for this cluster.

The next two isomers, (3-II) and (3-III), which are 0.60 and 1.36 kcal/mol higher in energy relative to the (3-I) global minimum, correspond to structures that have a different water network with respect to the homodromic[59] donor-acceptor (*da*) one found in the global minimum and the ion interacts with the water network via the N end. Two other isomers, labeled as (3-IV) and (3-V) in Fig. 4 and lying 1.40 kcal/mol and 1.62 kcal/mol above the global minimum, respectively, have the same water network with isomer (3-II) and (3-III), but differ in the fact that the ion interacts with the water network via the C end. The fact that those isomers lie higher in energy than (3-II) and (3-III) is consistent with the finding for the $n=2$ isomers, namely, that the $CN^-(H_2O)_2$ isomer is more stable than the $NC^-(H_2O)_2$ species.

In isomer (3-II) the three water molecules form a (*d′d-ad′a-dd′*) network whereas in isomer (3-III) the arrangement is (*d′a-dd-ad′*), where (*d′*) denotes a hydrogen bonding donor to the ion. The finding that the homodromic (*da-da-da*) network of isomer (3-I) is associated with the global minimum is consistent with the fact that it maximizes cooperativity,[59] whereas the energy ordering of isomers (3-II) and (3-III) is consistent with the observation that the more stable of the two (3-II) has an additional number of the stronger ion-water hydrogen bonds than the less stable one (3-III). A quantitative analysis of the relative energetics of these different networks can be performed by evaluating the individual two-, three-, and four-body terms,[60] involving the various moieties in the clusters.[33,58] However, this analysis goes beyond the scope of the present study, especially given the fact that the networks for (3-II) and (3-III) correspond to higher-lying isomers.

The experimental VDE of the $n=3$ cluster is 5.58 eV obtained from the T=12 K spectrum (Fig. 2). The calculated VDE of the global minimum (pyramidal isomer 3-I) is 5.74 eV at the MP2/aug-cc-pVDZ level. The use of a larger basis set will increase the calculated VDE, moving it away from the experimental value, since MP2 as a method overestimates this quantity [see point (iii) in Sec. II B]. Consistent with the results for the smaller clusters, the CCSD(T)/aug-cc-pVDZ//MP2/aug-cc-pVDZ VDE is 5.30 eV, which is 0.28

smaller than the experimental value. In addition, the corresponding VDE for structure TS3-I (which becomes the global minimum after zero-point energy corrections and is further stabilized at RT) is 5.29 eV, i.e., almost (within 0.01 eV) identical to the value for the 3-I isomer. When taking into account the ~0.2 eV increase in the VDE due to the basis set incompleteness at the CCSD(T) level, we estimate that the CCSD(T)/CBS value for both the 3-I and TS3-I configurations would lie within <0.1 eV from experiment. The MP2/aug-cc-pVDZ VDEs of isomers (3-II) and (3-III) are almost identical (5.65 and 5.67 eV), both being about 0.1 eV smaller than that of the global minimum (isomer 3-I). As regards the two higher lying isomers (3-IV) and (3-V), their MP2/aug-cc-pVDZ VDEs are computed at 5.81 and 5.82 eV, respectively. Therefore the broadening of the experimental peak toward low energy at RT can be rationalized in terms of the sampling of the 3-I, TS3-I (and possibly TS-II) configurations as well as those of isomers 3-II and 3-III.

### C. $CN^-(H_2O)_4$

We identified three minima on the PEF of the $CN^-(H_2O)_4$ cluster. The lowest energy structure (4-I) corresponds to the $CN^-$ interacting with a four water homodromic ring network in which each water molecule acts both as a donor and an acceptor to neighbors, resembling the structure of the gas phase water tetramer[56] (Fig. 5). As in the $n=3$ case the $CN^-$ anion lies almost parallel to the plane of the four Oxygen atoms. The two structures with $C_4$ symmetry (TS4-I and TS4-II in Fig. 6, having the N and C ends toward the water network) are both first order transition states with imaginary frequencies of 70.3 ($E$) and 26.0 $cm^{-1}$ ($E$), respectively. TS4-I lies 2.52 (1.79 with ZPE corrections) kcal/mol above 4-I, whereas TS4-II lies 4.13 (3.20) kcal/mol above 4-I. The corresponding enthalpy differences of the transition states with respect to 4-I at T=298 K are 1.16 (TS4-I) and 2.06 (TS-II) kcal/mol. Therefore, contrary to the $n=3$ case, zero-point and temperature do not stabilize the symmetric structures with respect to the global minima and the large amplitude motion corresponding to the tumbling of $CN^-$ with respect to the water network is less evident.

The calculated VDE at the MP2/aug-cc-pVDZ level for 4-I is 6.14 eV, whereas the CCSD(T)/aug-cc-pVDZ//MP2/aug-cc-pVDZ number is 5.67 eV. The latter is almost identical to the experimentally measured value of 5.89 eV when the basis set effect (~0.2 eV) is accounted for at the CCSD(T) level. The corresponding CCSD(T)/aug-cc-pVDZ//MP2/aug-cc-pVDZ VDE for TS4-I is 5.55 eV, a value that is ~0.15 eV away from experiment when the basis set correction of ~0.2 eV effect is added. For the $n=4$ cluster we note that the difference in the VDEs between the asymmetric and $C_4$ configurations is 0.12 eV, much larger than the 0.01 value previously found for the corresponding configurations of the $n=3$ cluster. The fact that the VDE of the global minimum (asymmetric configuration) is closer (within 0.02 eV) from experiment is consistent with the observed "quenching" of the tumbling of the $CN^-$ anion with respect to the water network.

The next isomer (4-II), which is 1.39 kcal/mol higher in energy, can be viewed as a three-water ring network interacting with the C end, while the fourth water molecule behaves like a double donor with one O–H···N H-bond to $CN^-$ and the other O–H···O H-bond to the three-water ring (4-II in Fig. 5). A third isomer (4-III) lying 1.49 kcal/mol above the global minimum can be considered as having the same water network with isomer (4-II) but with the $CN^-$ rotated by 180°. The structures of the (4-II) and (4-III) isomers resemble the isomers labeled as "3+1" for the $Cl^-(H_2O)_4$ cluster.[33] The VDEs of the two isomers are computed at the MP2/aug-cc-pVDZ level to be 6.32 and 6.24 eV, respectively, 0.18 and 0.10 eV larger than that of the global minimum (4-I).

## V. DISCUSSION

### A. Calculated electron binding energies of the global minima compared with the experiment

The electron binding energies of the hydrated $CN^-$ clusters directly reflect how this ion is solvated by the water molecules. Different structures and solvation environments are expected to give rise to different electron binding energies. Therefore, comparison of the calculated electron binding energies with the temperature-dependent PES spectra should provide information about the isomers populated at different temperatures and aid in identifying the global minimum structures. The calculated best values for the VDEs of the low-lying isomers of $CN^-(H_2O)_n$ ($n=2-4$) clusters are shown as broken vertical lines in Fig. 2 and listed in Table I. For the global minima the CCSD(T)/aug-cc-pVQZ for $n=0,1$ and the *basis-set-corrected* CCSD(T) for $n=2$, 3, and 4 (obtained by adding 0.2 eV to the CCSD(T)/aug-cc-pVDZ result) VDEs are shown in blue whereas the ones for the higher lying isomers are indicated in red (for $n=2$) in Fig. 2. Excellent agreement was observed between the best computed VDEs, 3.84 eV ($n=0$) and 4.54 eV ($n=1$), or the estimated VDEs for the larger clusters, 5.32 eV ($n=2$), 5.50 eV ($n=3$), and 5.87 eV ($n=4$), and the LT experimental values of 3.85 eV ($n=0$), 4.54 eV ($n=1$), 5.20 eV ($n=2$), 5.58 eV ($n=3$), and 5.89 eV ($n=4$), a result that lends considerable credence to the assignment of the lowest energy structures for each cluster. It also suggests that the CCSD(T) level of theory is capable of accurately predicting the corresponding VDEs for this system as long as a large basis set is used. In addition, the agreement between the *predicted* CCSD(T)/CBS limit VDEs and experiment lends further confidence to the scheme used to obtain those values for the larger clusters.

### B. Hydration motifs of the $CN^-(H_2O)_n$ clusters and comparison to $Cl^-(H_2O)_n$ and other aqueous diatomic anionic clusters

Being a model diatomic closed-shell anion, $CN^-$ is known to be able to interact with water via either the N or C atom ends, resulting in the formation of two nearly isoenergetic isomers, namely, $CN^-(H_2O)$ and $NC^-(H_2O)$, respectively.[15,17,19,22] Our recent joint PES and first principles electronic structure study[22] showed that the global minimum of the monohydrate corresponds to the $CN^-(H_2O)$ isomer, which is just 0.2 kcal/mol lower in energy than the corresponding $NC^-(H_2O)$ isomer at the CCSD(T)/aug-cc-pVQZ

level of theory including ZPE corrections. This assignment was supported by the excellent agreement (within $<0.01$ eV) between the calculated VDE for the $CN^-(H_2O)$ isomer and the experimental data, whereas the VDE of the $NC^-(H_2O)$ isomer was 0.13 larger.

Given the most stable arrangement of the $CN^-(H_2O)$ cluster, an additional water molecule can either bind to the C end of cyanide or form a cyclic structure by hydrogen bonding to the existing water molecule. Our calculations suggest that the former bonding scenario prevails in $CN^-(H_2O)_2$, resulting in isomer (2-I) as the global minimum, whereas the two isomers with interwater interactions (2-II and 2-III) lie 0.61 kcal/mol and 1.47 kcal/mol higher in energy. The structural motif observed for the $n=1$ cluster is also observed for $n=2$, namely, that the isomer in which the N end interacts with the water network (2-II) is lower in energy than the one in which the C atom interacts with the water network (2-III). It is interesting to note that in the case of the $Cl^-(H_2O)_2$ cluster the energetics of the two isomers are reversed with the highly symmetric linear structure lying 2.2 kcal/mol above the cyclic global minimum.[33]

With the addition of the third water molecule we observe the onset of hydrogen bonding between water molecules and the stabilization of water networks in the cluster structures. Because both binding sites of $CN^-$ are occupied in isomer (2-I), it is not advantageous to build $CN^-(H_2O)_3$ based on (2-I). Instead, the lowest energy structure of $CN^-(H_2O)_3$ (isomer 3-I) can be viewed as generated by adding the third water to the two-water network of (2-II) to form a three-water ring homodromic network ("pyramidal base"), where each water both donates and accepts one hydrogen bond from its neighbors. However, there is a large amplitude motion that corresponds to the free tumbling of the $CN^-$ anion on the surface of the water cluster with the "average" structure having $C_3$ symmetry (TS3-I, cf. Fig. 6). The next two low-lying isomers (3-II) and (3-III) can also be viewed to evolve from isomer (2-II) by adding a third water to form two extra water networks. Similarly, isomers (3-IV) and (3-V) are built starting from (2-III) and adding a third water to form water networks with different connectivity. Clearly, the water-water interactions prevail over the ion-water interaction when going from $CN^-(H_2O)_2$ to $CN^-(H_2O)_3$. Similar structures corresponding to the (3-I) and (3-III) isomers of $CN^-(H_2O)_3$ are also found for $Cl^-(H_2O)_3$.[33]

The global minimum and the two low-lying isomers of the $CN^-(H_2O)_4$ cluster all have clearly defined growth paths starting from isomer (3-I). Expanding the pyramidal water-ring base from three to four molecules and optimizing the solute interaction with this base leads to the global minimum isomer (4-I). This configuration is not destabilized with respect to the TS4-I transition state of $C_4$ symmetry (as in the $n=3$ case) although there is a similar trend of lowering the barriers at higher temperatures. On the other hand, having the three-water ring primarily interacting with one end of the $CN^-$ while the fourth water forms one H-bond with the other end of $CN^-$ and one interwater H-bond with the three-water ring yields isomers (4-II) and (4-III), respectively. Bonding configurations analogous to the (4-I) and (4-II) isomers were previously reported for the $Cl^-(H_2O)_4$ clusters[33]

It is instructive to compare the hydration motif of $CN^-(H_2O)_n$ with that of two other diatomic anionic clusters, $O_2^-(H_2O)_n$ (Refs. 35 and 36) and $NO^-(H_2O)_n$,[37] reported earlier, since significant differences are found. In particular, no cyclic water networks were observed for the larger $O_2^-(H_2O)_n$ $(n=3,4)$ clusters, whereas cyclic water trimers were reported in $NO^-(H_2O)_3$. This difference was rationalized, at least in part due to the different electron distributions of $O_2^-$ and $NO^-$, in terms of the presence or lack of cylindrical symmetry of the solvated anion. In the $O_2^-(H_2O)_n$ there is no cylindrical symmetry and the in-plane (defined by the ion and the first solvating water molecule) $\pi^*$ orbital is singly occupied whereas the out-of-plane $\pi^*$ orbital is doubly occupied. In contrast, due to the cylindrical symmetry for the $NO^-(H_2O)_n$ system, both orbitals are singly occupied. If we put the present case in the previously discussed perspective, $CN^-$ is a closed shell anion with cylindrical symmetry of the electron distribution. Its hydrated clusters examined in the present study show a solvation motif that is similar to that previously found for the $NO^-(H_2O)_n$ clusters, i.e., there exist dual H-bonding sites and cyclic water networks appear. A distinct difference, with respect to $NO^-(H_2O)_n$, in terms of the relative ordering of the low-lying isomers is also observed, i.e., the global minimum of $CN^-(H_2O)_2$ was found to be an open structure (2-I) with two individual $H_2O$ molecules solvating $CN^-$ from both ends, in contrast to a water dimerlike unit interacting with the solute ion previously reported for the $NO^-(H_2O)_2$ cluster (Ref. 37). Such a difference may also have an electronic origin since $CN^-$ is a closed shell ion whereas $NO^-$ is open shell one. A detailed study of the influence of the solutes electronic structure on the solvation morphology is certainly noteworthy to pursue.

### C. Temperature effects and temperature-dependent isomer population

As shown in Fig. 2, the spectra of the $CN^-(H_2O)_2$ and $CN^-(H_2O)_3$ clusters at RT are significantly broadened to the low binding energy side compared with the spectra at T $=12$ K. The VDEs measured from the RT spectra are 0.10 eV and 0.08 eV smaller than those obtained from the 12 K spectra for $n=2$ and 3, respectively (Table I). While it can be reasonably assumed that only the global minima are populated at T$=12$ K, low-lying isomers can also have appreciable contributions to the RT spectra. The (2-II) and (3-II) isomers are both only 0.6 kcal/mol above the (2-I) and (3-I) global minima, respectively, and should have significant populations at RT. The calculated VDEs for isomers (2-II) and (3-II) are lower by 0.26 eV and 0.09 eV, respectively, from the corresponding values for the global minima of the $n=2$ and $n=3$ clusters. These values lie within the observed broadening on the low binding energy side of the PES spectra. In contrast, the other isomers (2-III), (3-III)—(3-V) with their relative energies being $\geq 1.36$ kcal/mol above the lowest energy configurations, are not expected to have appreciable contributions at RT. The excitation of accessible soft vibrational modes at RT, which is the main reason for the observed spectral shift in the $n=1$ case (Ref. 22), may also

contribute to the spectral broadening and the shifts for the larger $n=2$ and 3 clusters in addition to the large amplitude motion for the tumbling of $CN^-$ on the surface of the water network found for $n=3$ and to a lesser extend for $n=4$.

## VI. CONCLUSIONS

We presented a joint *ab initio* electronic structure and photoelectron spectroscopic study on the hydration of the cyanide anion $CN^-(H_2O)_n$, $n=2-5$. The hydration of the $CN^-$ and $Cl^-$ ions is found to have many common elements as $CN^-$ is considered to be a pseudohalide and has a similar polarizability and hydration energy with $Cl^-$. Yet distinct differences were also found due to the existence of multiple hydrogen bonding sites for $CN^-$, namely, the lowest energy structure for $CN^-(H_2O)_2$ is a highly symmetric one with the two water molecules each forming H-bonding to the two ends of the solute and no interwater interactions, in contrast to the $Cl^-(H_2O)_2$ case.[34] For $n=3$ it was found that the anion can freely "tumble" on the surface of the water trimer and that this large amplitude motion is somewhat quenched for $n=4$. The existence of two hydrogen bond acceptor sites in $CN^-$ also produces a larger number of isomers than the corresponding halide-water clusters since there is now a choice of whether the cyanide ion interacts with the water network via the N or the C atom ends. In all cases the former isomers (N atom interacting with the water network) are more stable than the latter. Overall the water-water interactions prevail as larger clusters are formed resulting in structures in which the anion resides on the surface of a water cluster. This solvation motif is similar to the one previously suggested for the chloride[33,61] and bromide[61] anions and it is consistent with the fact that the ion-water interactions are of similar magnitude for those three anions, with fluoride being the exception forming "interior" structures[61–63] that are driven by the much larger (almost double) fluoride-water bond energy,[64] which overwhelms the water-water interactions. The comparison between $CN^-$ with other diatomic hydrated clusters also having cylindrical symmetry, such as $NO^-$, shows similar hydration motifs except for $n=2$ due to the different electronic configurations between the two anions ($CN^-$ being a closed, whereas $NO^-$ an open shell system). On the other hand, significant differences were found for other anions lacking cylindrical symmetry, such as $O_2^-$.

Excellent agreement between the calculated electron binding energies for the global minimum structures and the experimental values at T=12 K was observed. For $n=2$ and 3, the population at RT of the low-lying isomers lying within ~0.6 kcal/mol above the global minimum can contribute to the broadening of the RT PES spectra at the lower binding energy side. The current study further demonstrates that the delicate balance between ion-water and water-water interactions has a profound influence on the hydration structures of gaseous hydrated clusters. It is further noted that combining accurate theoretical calculations with the temperature-dependent PES technique is a valuable approach to unravel the stepwise hydration structures of complex anions.

## ACKNOWLEDGMENTS

This work was supported by the U. S. Department of Energy (DOE), Office of Basic Energy Sciences, Division of Chemical Sciences, Geosciences and Biosciences, and was performed at the Environmental Molecular Sciences Laboratory (EMSL), a national scientific user facility sponsored by DOE's Office of Biological and Environmental Research and located at Pacific Northwest National Laboratory, which is operated by Battelle for the DOE. Computer resources were provided at the Molecular Science Computing Facility (MSCF) in EMSL.

[1] F. A. Cotton, G. Wilkinson, C. A. Murillo, and M. Bochmann, *Advanced Inorganic Chemistry*, 6th ed. (Wiley, New York, 1999).
[2] S. E. Bradforth, E. H. Kim, D. W. Arnold, and D. M. Neumark, J. Chem. Phys. **98**, 800 (1993).
[3] R. Klein, R. P. McGinnis, and S. R. Leone, Chem. Phys. Lett. **100**, 475 (1983).
[4] J. Berkowitz, W. A. Chupka, and T. A. Walter, J. Chem. Phys. **50**, 1497 (1969).
[5] D. Forney, W. E. Thompson, and M. E. Jacox, J. Chem. Phys. **97**, 1664 (1992).
[6] P. W. Fowler and M. L. Klein, J. Chem. Phys. **85**, 3913 (1986).
[7] M. Ferrario, I. R. McDonald, and M. L. Klein, J. Chem. Phys. **84**, 3975 (1986).
[8] M. Koziński, S. Garrett-Roe, and P. Hamm, Chem. Phys. **341**, 5 (2007).
[9] Q. Zhong, A. P. Baronavski, and J. C. Owrutsky, J. Chem. Phys. **119**, 9171 (2003).
[10] M. Shiga and S. Okazaki, J. Chem. Phys. **111**, 5390 (1999).
[11] R. Rey and J. T. Hynes, J. Chem. Phys. **108**, 142 (1998).
[12] E. J. Heilweil, F. E. Doany, R. Moore, and R. M. Hochstrasser, J. Chem. Phys. **76**, 5632 (1982).
[13] J. D. Payzant, R. Yamdagni, and P. Kebarle, Can. J. Chem. **49**, 3308 (1971).
[14] J. W. Larson, J. E. Szulejko, and T. B. McMahon, J. Am. Chem. Soc. **110**, 7604 (1988).
[15] J. W. Larson and T. B. McMahon, J. Am. Chem. Soc. **109**, 6230 (1987).
[16] M. Meot-Ner, S. M. Cybulski, S. Scheiner, and J. F. Liebman, J. Phys. Chem. **92**, 2738 (1988).
[17] T. J. Lee, J. Am. Chem. Soc. **111**, 7362 (1989).
[18] J. Gao, D. S. Garner, and W. L. Jorgensen, J. Am. Chem. Soc. **108**, 4784 (1986).
[19] T. Ikeda, K. Nishimoto, and T. Asada, Chem. Phys. Lett. **248**, 329 (1996).
[20] L. X. Dang, J. Phys. Chem. B **106**, 10388 (2002).
[21] T. R. Miller, in *CRC Handbook of Chemistry and Physics*, 72nd ed., edited by D. R. Lide (CRC, Cleveland, 1991), pp. 10–180.
[22] X. B. Wang, J. C. Werhahn, L. S. Wang, K. Kowalski, A. Laubereau, and S. S. Xantheas, J. Phys. Chem. A **113**, 9579 (2009).
[23] X. B. Wang, X. Yang, J. B. Nicholas, and L. S. Wang, Science **294**, 1322 (2001).
[24] J. M. Papanikolas, J. R. Gord, N. E. Levinger, D. Rat, V. Vorsa, and W. C. Lineberger, J. Phys. Chem. **95**, 8028 (1991).
[25] D. J. Miller and J. M. Lisy, J. Am. Chem. Soc. **130**, 15381 (2008); O. M. Cabarcos, C. J. Weinheimer, and J. M. Lisy, J. Chem. Phys. **110**, 8429 (1999).
[26] G. Markovich, S. Pollack, R. Giniger, and O. Cheshnovsky, J. Chem. Phys. **101**, 9344 (1994).
[27] L. Lehr, M. T. Zanni, C. Frischkorn, R. Weinkauf, and D. M. Neumark, Science **284**, 635 (1999).
[28] N. R. Walker, R. S. Walters, M. K. Tsai, K. D. Jordan, and M. A. Duncan, J. Phys. Chem. A **109**, 7057 (2005).
[29] A. Stace, Science **294**, 1292 (2001); H. Cox, G. Akibo-Betts, R. R. Wright, N. R. Walker, S. Curtis, B. Duncombe, and A. J. Stace, J. Am. Chem. Soc. **125**, 233 (2003).
[30] J. H. Choi, K. T. Kuwata, Y. B. Cao, and M. Okumura, J. Phys. Chem. A **102**, 503 (1998).
[31] P. Ayotte, G. H. Weddle, J. Kim, and M. A. Johnson, J. Am. Chem. Soc. **120**, 12361 (1998).
[32] E. G. Diken, J. M. Headrick, J. R. Roscioli, J. C. Bopp, M. A. Johnson, A. B. McCoy, X. Huang, S. Carter, and J. M. Bowman, J. Phys. Chem. A

**109**, 571 (2005).
[33] S. S. Xantheas, J. Phys. Chem. **100**, 9703 (1996).
[34] H. E. Dorsett, R. O. Watts, and S. S. Xantheas, J. Phys. Chem. A **103**, 3351 (1999).
[35] J. M. Weber, J. A. Kelley, S. B. Nielsen, P. Ayotte, and M. A. Johnson, Science **287**, 2461 (2000).
[36] J. M. Weber, J. A. Kelley, W. H. Robertson, and M. A. Johnson, J. Chem. Phys. **114**, 2698 (2001).
[37] E. M. Myshakin, K. D. Jordan, W. H. Robertson, G. H. Weddle, and M. A. Johnson, J. Chem. Phys. **118**, 4945 (2003).
[38] E. A. Price, N. I. Hammer, and M. A. Johnson, J. Phys. Chem. A **108**, 3910 (2004).
[39] W. H. Robertson, E. A. Price, J. M. Weber, J.-W. Shin, G. H. Weddle, and M. A. Johnson, J. Phys. Chem. A **107**, 6527 (2003).
[40] E. M. Myshakin, K. D. Jordan, E. L. Sibert III, and M. A. Johnson, J. Chem. Phys. **119**, 10138 (2003).
[41] O. V. Boyarkin, S. R. Mercier, A. Kamariotis, and T. R. Rizzo, J. Am. Chem. Soc. **128**, 2816 (2006).
[42] J. Zhou, G. Santambrogio, M. Brümmer, D. T. Moore, L. Wöste, G. Meijer, D. M. Neumark, and K. R. Asmis, J. Chem. Phys. **125**, 111102 (2006).
[43] M. F. Bush, R. J. Saykally, and E. R. Williams, J. Am. Chem. Soc. **129**, 2220 (2007).
[44] X. B. Wang, J. Yang, and L. S. Wang, J. Phys. Chem. A **112**, 172 (2008).
[45] X. B. Wang, A. P. Sergeeva, J. Yang, X. P. Xing, A. I. Boldyrev, and L. S. Wang, J. Phys. Chem. A **113**, 5567 (2009); X. B. Wang, B. Jagoda-Cwiklik, C. Chi, X. P. Xing, M. Zhou, P. Jungwirth, and L. S. Wang, Chem. Phys. Lett. **477**, 41 (2009).
[46] X. B. Wang, H. K. Woo, L. S. Wang, B. Minofar, and P. Jungwirth, J. Phys. Chem. A **110**, 5047 (2006); X. B. Wang, H. K. Woo, B. Kiran, and L. S. Wang, Angew. Chem., Int. Ed. **44**, 4968 (2005).
[47] A. L. Nicely, D. J. Miller, and J. M. Lisy, J. Am. Chem. Soc. **131**, 6314 (2009).
[48] X. B. Wang and L. S. Wang, Rev. Sci. Instrum. **79**, 073108 (2008).
[49] L. S. Wang, C. F. Ding, X. B. Wang, and S. E. Barlow, Rev. Sci. Instrum. **70**, 1957 (1999).
[50] T. H. Dunning, Jr., J. Chem. Phys. **90**, 1007 (1989); R. A. Kendall, T. H. Dunning, Jr., and R. J. Harrison, *ibid.* **96**, 6796 (1992).
[51] M. J. Frisch, G. W. Trucks, H. B. Schlegel *et al.*, GAUSSIAN98, Revision A.9, Gaussian, Inc., Pittsburgh, PA, 1998.
[52] R. A. Kendall, E. Aprà, D. E. Bernholdt, E. J. Bylaska, M. Dupuis, G. I. Fann, R. J. Harrison, J. Ju, J. A. Nichols, J. Nieplocha, T. P. Straatsma, T. L. Windus, and A. T. Wong, Comput. Phys. Commun. **128**, 260 (2000); High Performance Computational Chemistry Group, *NWChem, A Computational Chemistry Package for Parallel Computers, Version 4.6* (Pacific Northwest National Laboratory, Richland, WA, 2003).
[53] S. J. Hirata, J. Phys. Chem. A **107**, 9887 (2003).
[54] (a) G. D. Purvis III and R. J. Bartlett, J. Chem. Phys. **76**, 1910 (1982); (b) K. Raghavachari, G. W. Trucks, J. A. Pople, and M. Head-Gordon, Chem. Phys. Lett. **157**, 479 (1989).
[55] M. Schütz, T. Bürgi, S. Leutwyler, and H. B. Bürgi, J. Chem. Phys. **99**, 5228 (1993).
[56] S. S. Xantheas and T. H. Dunning, Jr., J. Chem. Phys. **98**, 8037 (1993); **99**, 8774 (1993).
[57] S. S. Xantheas and T. H. Dunning, Jr., J. Phys. Chem. **96**, 7505 (1992).
[58] S. S. Xantheas, J. Am. Chem. Soc. **117**, 10373 (1995).
[59] S. S. Xantheas, Chem. Phys. **258**, 225 (2000).
[60] S. S. Xantheas, J. Chem. Phys. **100**, 7523 (1994).
[61] P. Ayotte, S. B. Nielsen, G. H. Weddle, M. A. Johnson, and S. S. Xantheas, J. Phys. Chem. **103**, 10665 (1999).
[62] S. S. Xantheas and L. X. Dang, J. Phys. Chem. **100**, 3989 (1996).
[63] O. M. Cabarcos, C. J. Weinheimer, J. M. Lisy, and S. S. Xantheas, J. Chem. Phys. **110**, 5 (1999).
[64] P. Weis, P. R. Kemper, M. T. Bowers, and S. S. Xantheas, J. Am. Chem. Soc. **121**, 3531 (1999).